Structural and optical study of Ce segregation in Ce-doped SiO 1.5 thin films

Georges Beainy, Jennifer Weimmerskirch-Aubatin, Mathieu Stoffel, M. Vergnat, Hervé Rinnert, Celia Castro, Philippe Pareige, Etienne Talbot

JOURNAL OF APPLIED PHYSICS **118**, 234308 (2015)

Structural and optical study of Ce segregation in Ce-doped $SiO_{1.5}$ thin films

G. Beainy,[1] J. Weimmerskirch-Aubatin,[2] M. Stoffel,[2] M. Vergnat,[2] H. Rinnert,[2] C. Castro,[1] P. Pareige,[1] and E. Talbot[1,a)]

[1]*Groupe de Physique des Matériaux, Université et INSA de Rouen, UMR CNRS 6634, Normandie Université, Avenue de l'Université, BP 12, 76801 St Etienne du Rouvray, France*

[2]*Université de Lorraine, UMR CNRS 7198, Institut Jean Lamour, BP 70239, 54506 Vandoeuvre-lès-Nancy, France*

(Received 1 October 2015; accepted 4 December 2015; published online 18 December 2015)

Cerium doped $SiO_{1.5}$ thin films fabricated by evaporation and containing silicon nanocrystals were investigated by atom probe tomography. The effect of post-growth annealing treatment has been systematically studied to correlate the structural properties obtained by atom probe tomography to the optical properties measured by photoluminescence spectroscopy. The atom probe results demonstrated the formation of Ce-Si rich clusters upon annealing at 900 °C which leads to a drastic decrease of the Ce-related luminescence. At 1100 °C, pure Si nanocrystals and optically active cerium silicate compounds are formed. Consequently, the Ce-related luminescence is found to re-appear at this temperature while no Si-nanocrystal related luminescence is observed for films containing more than 3% Ce. © *2015 AIP Publishing LLC*. [http://dx.doi.org/10.1063/1.4938061]

I. INTRODUCTION

During the last decades, silicon (Si) integrated photonics has attracted much interest due to the increasing demand of optical devices such as light emitting diodes or optical interconnects. These devices could be integrated together with microelectronic functionalities on the same Si substrate. Unfortunately, the presence of an indirect band gap in bulk silicon makes it a poor light emitter and has prevented its application as a light source for integrated optoelectronics. Since the discovery of photoluminescence of porous silicon by Canham[1] in 1990, it has been found that nanostructured silicon materials can emit light at room temperature in the visible-near infrared. Although an optical gain was claimed with systems containing silicon nanocrystals (Si-ncs),[2,3] there is still no efficient light emitting device available based on Si-ncs. The main drawback is that the emission of Si-ncs is rather weak and is limited to a narrow spectral range between 600 and 850 nm.

Doping silicon-based materials with optically active ions can be a promising route to circumvent this problem. Rare-earth doped SiO_X $(0 < X < 2)$ films containing Si-ncs are attracting particular interest since they may extend the functionalities and applications of silicon in optoelectronics. Among the rare earth elements, erbium has received a considerable attention during the last years due to its coincidence with the low loss window in optical fiber communication systems. It has been found that silicon nanocrystals can act as sensitizers for the emission of erbium[4,5] and neodymium.[6] However, in order to get a silicon based light emitting device covering the visible range, other rare earth elements should be considered. In this work, we investigate Ce-doped $SiO_{1.5}$ thin films containing Si nanocrystals. Cerium is of particular interest since Ce^{3+} is characterized by an electric dipolar allowed $5d - 4f$ transition leading to emission in the violet-blue.

Characteristic violet/blue luminescence has been reported from cerium oxide films grown by pulsed laser deposition[7] or by radio-frequency sputtering on silicon substrates.[8] The observed luminescence was attributed either to the formation of cerium oxide such as Ce_6O_{11} or silicate phases ($Ce_2Si_2O_7$ or $Ce_{4.667}(SiO_4)_3O$). Li *et al.*[9] investigated the optical properties of Ce-doped silicon oxide thin films grown by electron resonance plasma enhanced chemical vapor deposition. The strongest luminescence has been observed on the sample annealed at 1200 °C due to the formation of cerium silicates. Many other works have also concerned Ce-doped silica glasses prepared by the sol-gel technique.[10–13] Moreover, Cong *et al.*[14] have studied Ce-doped silica films prepared by ion-beam sputtering and ion implantation. These authors mentioned the strong dependence of the luminescence properties on the Ce concentrations and annealing conditions. Indeed, the rare earth based light emission is strongly dependent on the microstructure such as dopant concentration, clustering, and their distributions in the host matrix.

Up to now, conventional techniques, such as Transmission Electron Microscopy (TEM),[15] Photoluminescence (PL), or fluorescence of extended X-ray absorption fine structure spectroscopy (EXAFS),[16,17] were used in order to investigate rare earth elements in SiO_x films. These techniques do not offer a direct access to the chemical distribution and compositions of the studied elements. While extensive work has been already performed on Ce-doped silica, Ce-doped silicon rich silicon oxide system has not been entirely considered yet. Furthermore, a systematic investigation of the effect of annealing temperature on the spatial distributions of Ce and Si atoms, their spatial relationships, and their precipitation kinetics is still lacking. Our overall objective is to perform a deep investigation on such effect and to describe the complex precipitation mechanism in Ce-doped in $SiO_{1.5}$ films. Atom Probe Tomography (APT) has emerged as a unique technique that is able to provide

a)Electronic mail: etienne.talbot@univ-rouen.fr

information about the chemical composition of elements together with a 3D map indicating the position of each atom from a specimen at the atomic scale thus allowing a complete picture of nanostructural evolution. The distribution and the evolution of the Ce phases and of Si-ncs were investigated for both as-deposited and annealed films. Finally, the nanostructural properties were correlated to the optical properties of the films. The purpose of this paper is to perform a deep analysis of Ce-doped $SiO_{1.5}$ thin films by means of APT experiments.

II. EXPERIMENTAL SECTION

The Ce-doped $SiO_{1.5}$ thin films were prepared by co-evaporation on a Si (001) substrate maintained at room temperature of SiO powder from a thermal cell and SiO_2 powder from an e-beam gun in an ultra-high vacuum chamber. The Ce doping was performed using a Kundsen cell heated at ~1400 °C. The Ce concentration defined as [Ce]/([Ce] + [Si] + [O]) was estimated to 3 at. %. The film thickness was monitored by a quartz microbalance and was 200 nm. All samples were post-grown annealed at different temperatures in either a tubular oven at 900°C for 1 h in vacuum or in a rapid thermal annealing furnace in N_2 atmosphere at 980 °C and 1100 °C during 5 min. The optical properties were investigated by steady state PL spectroscopy using a 260 nm laser as excitation. For APT experiments, the sample must be shaped into a sharp tip with a curvature radius less than 50 nm to facilitate surface evaporation. In this work, Ce-doped $SiO_{1.5}$ tiny needles were prepared by using focused ion beam annular milling procedure with Ga ions. The details of this standard procedure are reported in another work[18] and were previously applied on Er-doped silicon oxide samples.[19] In order to prevent the implantation of any Ga ions during the milling process, a 350 nm thick platinum layer is deposited on the top of the sample and, at final stage a low accelerating voltage (2 kV) was used. The prepared tips have an end radius close to 30 nm. APT experiments are carried out with a Laser Assisted Wide Angle Tomographic Atom Probe (LAWATAP-CAMECA). With this technique, surface atoms are emitted from the tip in the form of ions by first establishing an intense electric field ($V_{DC} \sim 5$–15 kV) below the ionization threshold of the sample and then by applying a short duration laser pulse that triggers the ion evaporation from the tip surface. Before the analysis, the specimen was cooled down to 80 K. The experiment is then performed in the analysis chamber with a vacuum of 2×10^{-10} mbar and with UV ($\lambda = 343$ nm) femtosecond laser pulses. In order to further confirm the APT results a piece from the sample annealed at 1100 °C was prepared for transmission electron microscopy observations. A plan-view has been obtained by mechanical polishing and Ar ion milling. High-resolution TEM (HR-TEM) and Energy Filtered TEM (EFTEM) experiments have been performed on a JEOL-ARM200F working at 120 kV and equipped with a Gatan imaging filter Quantum ER.

III. RESULTS AND DISCUSSION

In an APT experiment, the first aspect to be considered is the mass spectrometry which is used to determine the mass over charge ratio of each evaporated ion, thus enabling its elemental identification. Figure 1 presents a typical mass spectrum of a 3 at. % Ce-doped $SiO_{1.5}$ film obtained in an APT experiment. Each significant peak is associated to a specific element or molecule. As shown, only the three expected chemical elements (Si, O, and Ce) with their isotopes and their molecular ions were found in the samples. Each atomic species can be detected in different charged states. Silicon is identified as Si^{3+}, Si^{2+}, and Si^{1+} and as molecular ions SiO^{2+}, SiO^{1+}, SiO_2^{2+}, and SiO_2^{1+}. Oxygen is found as single element O^{2+} and as molecular ions O_2^{2+} and O_2^{1+}. The detected oxygen peak at 16 a.m.u can be attributed either to O_2^{2+} or O_1^{1+}. Previous studies on silicon oxide systems[19,20] show a good composition agreement by considering it as O_2^{2+}. Finally, cerium ions are detected as Ce^{3+}, Ce^{2+}, and CeO^{2+}. We note here that the charge state of ions can be explained by the evaporation mechanism of APT. It is not related to the valence state of the atom; therefore, APT does not allow discriminating between Ce^{3+} and Ce^{4+} ions in the sample. The mean chemical composition of the samples was simply computed from the proportions of atoms of each species. For all the analyzed samples, no significant change in the mean composition is observed. A mean composition of 41.50 ± 0.06 at. % in Si, 56.10 ± 0.06 at. % in O, and 2.40 ± 0.02 at. % in Ce is obtained. This corresponds to a concentration of 1.6×10^{21} at. cm^{-3} of Ce and a silicon in excess of 13.5 at. % which is in good agreement with that expected from fabrication conditions.

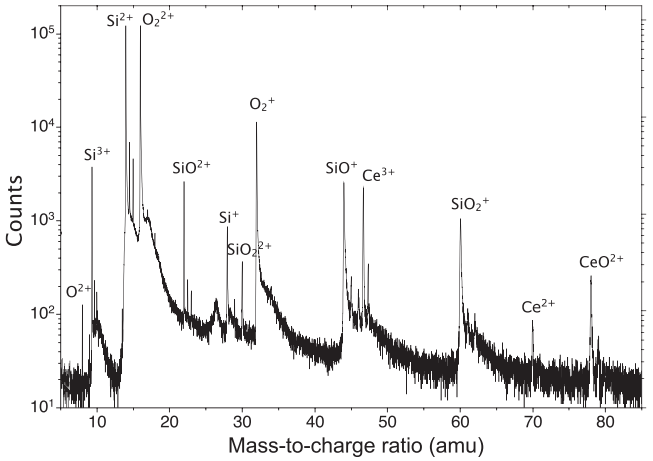

FIG. 1. Atom probe tomography mass spectrum obtained on Ce-doped $SiO_{1.5}$ films.

Figure 2 shows cross-sectional views of the 3D reconstructed volume obtained by the APT analysis of both as-deposited and annealed Ce-doped $SiO_{1.5}$ films. For the as-deposited layer (Figure 2(a)), the 3D reconstruction of the analyzed volume reveals that Si atoms are homogeneously distributed. This was confirmed by a statistical test of randomness described by Thuvander *et al.*[21] (not presented here). In contrast, Ce atoms are clearly inhomogeneously distributed. When the sample is annealed at 900 °C, Si atoms diffuse to Ce-inhomogeneous areas to form Si-Ce rich clusters containing also O (not presented here for the sake of clarity) (Figure 2(b)). Moreover, no clear evidence of Ce diffusion is observed. When the temperature rises from 900 °C

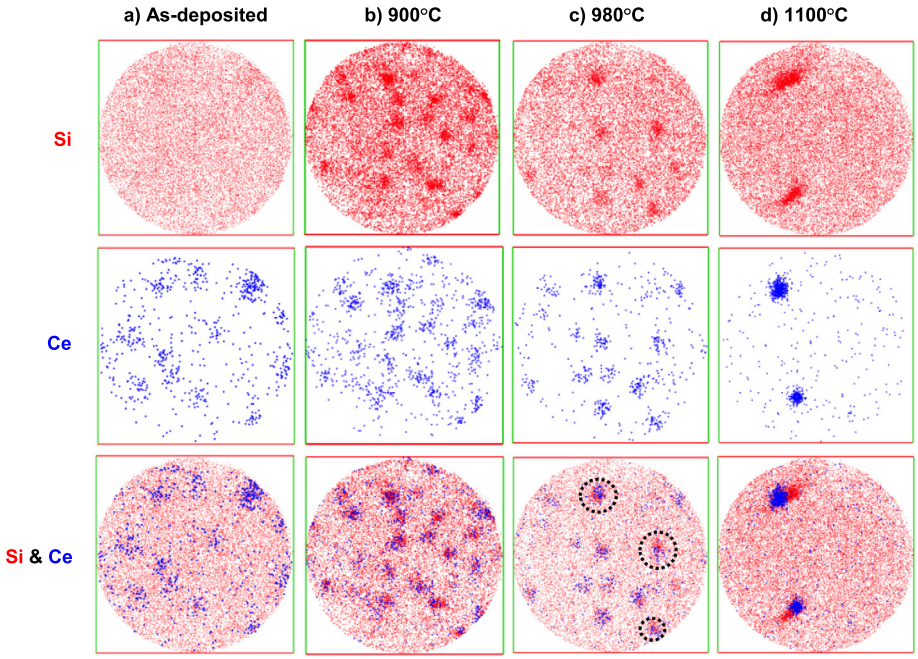

FIG. 2. Cross-sections of the 3D reconstructed volume obtained from APT analysis of the as-deposited (a) and annealed at various temperatures ((b) 900 °C, (c) 980 °C, and (d) 1100 °C) layers for Ce-doped $SiO_{1.5}$ samples. Volumes: $24 \times 24 \times 5\,nm^3$. For clarity, oxygen atoms are not shown.

to 980 °C, Si-Ce rich clusters still present, but we can notice the beginning of a phase separation between pure Si and Ce rich clusters. Si atoms seem to be ejected from these Si-Ce rich clusters (see dashed-circle in Figure 2(c)). After 1100 °C annealing, Ce-rich and pure Si clusters are well separated with a smaller density compared to samples annealed at lower temperatures (Figure 2(d)). The mean composition of the Ce-rich clusters was quantified by measurements made owing to boxes placed well inside the observed clusters (so-called in-core measurements).

All the measured compositions of individual Ce-rich clusters are reported in Figure 3, which represents the Si-O-Ce phase diagram. For the as-deposited, 900 and 980 °C annealed samples, the composition of the Ce-rich clusters exhibits a rather large dispersion and does not correspond to a stable phase. For the sample annealed at 1100 °C, the mean composition of the Ce-rich clusters is $X_{Ce} = 16.3 \pm 0.4$ at. %, $X_{Si} = 18.2 \pm 0.4$ at. %, and $X_O = 65.5 \pm 0.4$ at. % which can be attributed to the Ce-silicate phase $Ce_2Si_2O_7$. However, one cannot exclude the formation of the compound $Ce_{4.667}(SiO_4)_3O$ which can coexist with $Ce_2Si_2O_7$ phase as mentioned in the literature.[8,9,22] Moreover, the measured composition shows first an increase of the Si content with a constant Ce composition (~7%–8%) between as-deposited and 900 °C annealing (in agreement with Figure 2(b)). Annealing at 980 °C leads to a Ce enrichment while the Si content decreases (Figure 2(c)). Equilibrium concentration of Ce silicate $Ce_2Si_2O_7$ phase was obtained at 1100 °C.

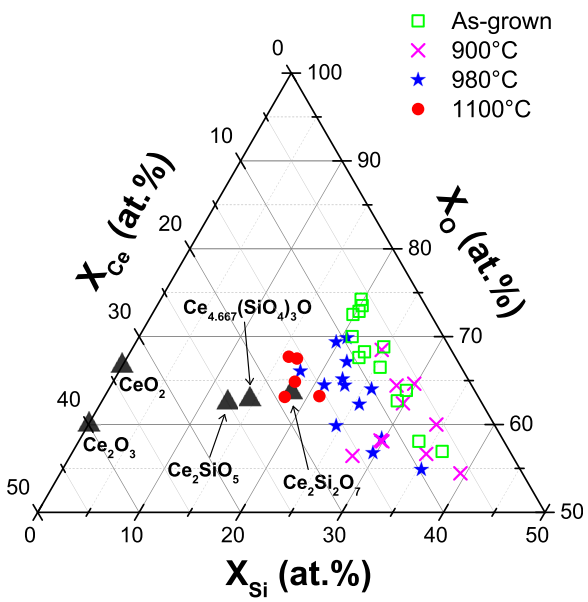

FIG. 3. APT measurements of the Ce-rich areas reported in ternary Si-O-Ce phase diagram for as-deposited and annealed samples.

The 3D reconstruction obtained on the sample annealed at 1100 °C is presented in Figure 4. Surprisingly, it shows that all Ce-silicates clusters are located in the vicinity of pure Si-ncs. The mean radius of Si-ncs and Ce-silicate clusters were measured to be $\langle r_{Si} \rangle = 1.7 \pm 0.4$ nm and $\langle r_{Ce} \rangle = 2.5 \pm 0.3$ nm, respectively, and with the same density of about $2.4 \times 10^{17}\,cm^{-3}$. Moreover, the clusters' density is lower for the samples annealed at lower temperatures than that of 1100 °C. This observation suggests that growth of Ce-silicates and pure Si clusters takes place at 1100 °C. Similar behavior has been already shown on Er-doped silicon rich silica by Talbot *et al.*[19] This fact can be related to the early stages of phase separation between Si in excess and SiO_2 matrix. In our samples, Si, which was initially homogeneously distributed in the as-deposited sample (as seen in Figure 2), diffuses to form Si-Ce-O clusters at 900 °C. These clusters do not correspond to any stable compound and are not thermodynamically stable. Therefore, at 1100 °C, the system tends to stabilize by ejection and self-assembling of Si atoms which leads to the formation of $Ce_2Si_2O_7$ phase and pure Si-ncs. In undoped silicon rich silicon oxide,[20,23] the phase separation occurs at high temperature where all Si atoms in excess precipitate to form pure Si-ncs and SiO_2

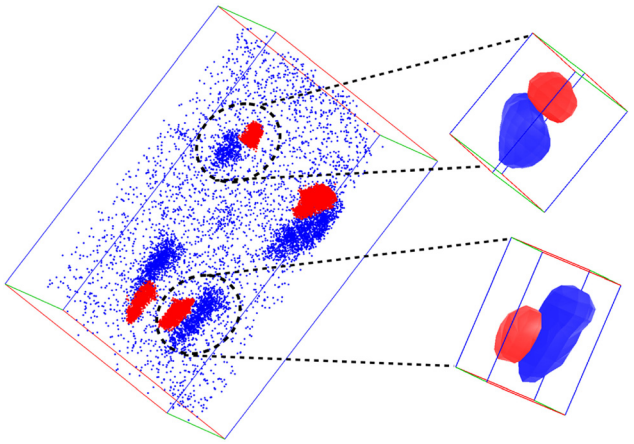

FIG. 4. 3D reconstruction of 1100 °C annealed Ce-doped $SiO_{1.5}$ film. The blue dots correspond to Ce atoms in the analyzed volume while the red ones correspond to Si-ncs. The insets represent an iso-concentration surface on Ce (blue) and Si (red) obtained for $X_{Ce} > 10\%$ and $X_{Si} > 70\%$, respectively. Volume: $25 \times 25 \times 40\,nm^3$.

matrix. In our study, Si in excess is found to be either in $Ce_2Si_2O_7$ phase or in Si-ncs. The Si nanoclusters growth mechanism is clearly modified by the presence of Ce-dopants in the sample. Moreover, at 1100 °C, the matrix is composed of pure SiO_2 and diluted Ce atoms which are not belonging to the silicate clusters. This indicates that, after 1100 °C annealing step, all the amount of Si in excess belongs to either $Ce_2Si_2O_7$ or to Si-ncs. The atomic fraction (f_a^{Ce}) of Ce atoms in the clusters is defined as the ratio of Ce atoms in $Ce_2Si_2O_7$ phase (N_{Ce}^C) over the total number of Ce atoms (N_{Ce}^T) by the following formula:

$$f_a^{Ce} = \frac{N_{Ce}^C}{N_{Ce}^T}. \quad (1)$$

Following this equation, the atomic fraction is estimated to be $f_a^{Ce} = 54\%$. This suggests that about 46% of the Ce ions remain in the matrix as isolated ions while the rest (54%) of the Ce ions belongs to the cerium silicate phase ($Ce_2Si_2O_7$).

In order to confirm the observed microstructure, HRTEM and EFTEM experiments have been performed on the 1100 °C annealed sample. Figure 5(a) shows the plane view HRTEM image. The bright and dark contrasts are associated with the formation of Si-ncs and Ce-rich phases, respectively. Some Si-ncs appear to be crystallized which is consistent with the previous studies on Si-ncs embedded in a SiO_2 matrix.[24,25] The EFTEM images of the Si plasmon peak and of the Ce $N_{4,5}$ core-loss edge are superimposed in Figures 5(b) and 5(d) and 5(c) and 5(d), respectively. The Si EFTEM image was obtained by filtering within a window at 17 ± 2 eV which is a characteristic of the plasmon loss energy of Si-ncs embedded in silica.[26] The analysis shows that Si-ncs appear as bright regions while dark regions are identified in their immediate vicinity. These dark regions correspond to cerium rich zones as shown in Figure 5(c) which has been obtained by filtering at an energy loss of 125 eV characteristic of oxidized Ce.[27] As a consequence, both APT and TEM confirm that pure Si-ncs and Ce-rich clusters are well formed in our sample and are connected to each other. The size distribution of the detected particles is in good agreement with that detected in APT. Moreover, TEM images show almost circular clusters which imply that the particles in the sample are spherical. However, the elongated shape of the clusters observed by APT (Figure 4) is due to local magnification effect during atom probe experiments.[28] Such an effect affects only the shape of the spherical nanoparticles in the analysis direction and does not affect composition measurements or size.

Figure 6 reports the room temperature steady-state PL spectra of both as-grown and annealed Ce-doped $SiO_{1.5}$ films at 900 °C, 980 °C, and 1100 °C. For all samples, a unique contribution in the blue region is observed. The luminescence can be attributed to the electric dipolar allowed 5d–4f transitions of Ce^{3+} ions. For all annealing temperature considered in this study, the PL spectra appear rather broad extending from 350 nm to at least 600 nm. Moreover, it is clearly seen that annealing at 900 °C and 980 °C leads to a drastic decrease of the Ce^{3+} PL emission which becomes almost negligible. Further annealing from 980 °C to 1100 °C leads to a significant increase of the PL intensity. In the case of Ce, the 5d orbitals are delocalized and are thus highly sensitive to the crystal field. As the annealing temperature increases, the local environment of the Ce^{3+} ions changes in the host matrix thus leading to a shift and/or a shape change of the Ce-related PL peak. The 1100 °C annealed sample exhibits the highest PL intensity. It reflects a totally different chemical environment of Ce^{3+} ions in the matrix. We further note that we do not observe any Si-nc related PL peak near 800 nm for the 3% Ce-doped $SiO_{1.5}$ thin film.

Let us correlate now the mentioned PL to the observed microstructure. For the as-deposited layer, the Ce-emission derives from the distributed Ce^{3+} ions in the sample. After annealing at 900 °C and 980 °C, the PL intensity drops sharply. The Ce mapping obtained by APT for these temperatures (Figure 2) displays that Ce ions are heterogeneous but more remarkably than for the as-deposited sample. The quenching of the Ce-related luminescence is then related to the clustering of cerium ions. No stable compound was detected at these temperatures. We note that PL spectra measured at 900 °C and 980 °C are very similar in shape and position which is consistent with the APT results indicating that the chemical environment of Ce ions does not change significantly. Thus, the Ce-related emission is quenched due to non-radiative energy transfer between neighboring Ce ions.[29] The surprising reappearance of the PL emission at 1100 °C is the result of the formation of Ce-silicate phase ($Ce_2Si_2O_7$). Moreover, the PL peak position shifts due to a different chemical environment of Ce ions in the above mentioned compounds. The latter shows luminescence around 400 nm which is compatible with our PL measurements.[8,30] It is noteworthy that the emission intensity from $Ce_2Si_2O_7$ clusters is very strong although the size of the nanostructures identified by APT analyses is rather small. It seems that cerium silicates provide an efficient way to reach a high density of trivalent Ce ions without suffering from ion-ion interactions, which typically impose an upper limit for the optimal concentration of a rare earth dopant in silicon oxide films. The bonding structure in the $Ce_2Si_2O_7$ lattice ensures

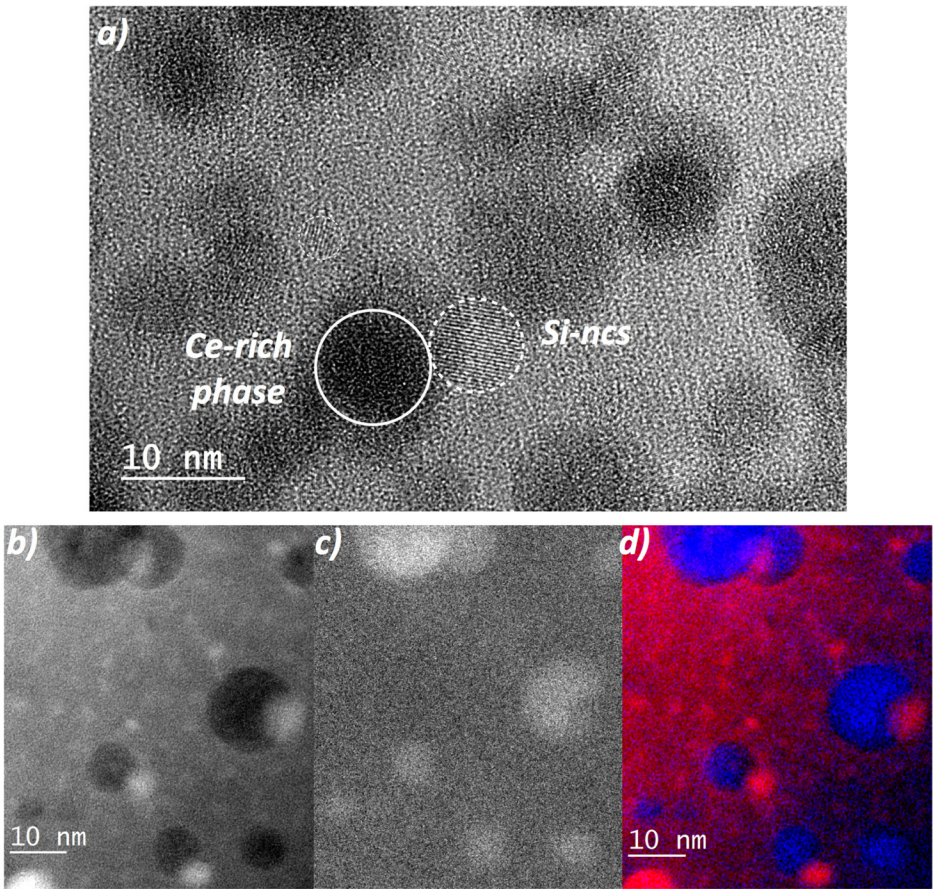

FIG. 5. TEM images on the 1100 °C Ce-doped $SiO_{1.5}$ film. (a) Plane view HRTEM. EFTEM images of (b) silicon, (c) cerium, and (d) color map within Si in red and Ce in blue.

that all cerium ions in the nanostructure are optically active and emit at the same wavelength providing excellent blue emission at room temperature. Moreover, it should be noted that $Ce_2Si_2O_7$ can exist in various polymorphs.[30] In our samples, we are not able to identify the $Ce_2Si_2O_7$ polymorph or to confirm if only one polymorph is present. In contrast, the PL spectra show that no luminescence from Si-ncs is observed although Si-ncs are clearly identified in the APT analysis for the sample annealed at 1100 °C. The mean radius of the Si-ncs mentioned before is in the order of 1.7 nm which is compatible with charge carrier confinement and subsequent light emission. Recently, a work done by Weimmerskirch-Aubatin *et al.*[31] on similar system has shown that there is no energy transfer between Si-ncs and Ce^{3+} ions. The absence of Si-nc related luminescence may thus be explained by the fact that Si-ncs are located nearby cerium silicates, which probably provide non-radiative recombination pathways.

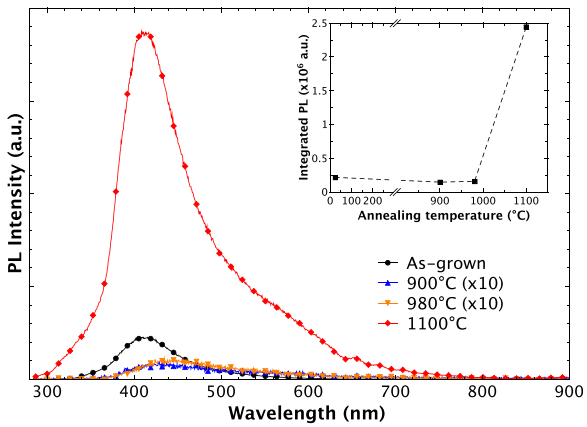

FIG. 6. Room temperature steady-state PL spectra for the as-grown Ce-doped $SiO_{1.5}$ layer and annealed at 900 °C, 980 °C, and 1100 °C. The inset shows the integrated PL intensity as a function of annealing temperature.

IV. CONCLUSION

In this work, we investigated the nanostructure of Ce-doped silicon-rich silica at the atomic level by APT and TEM. The obtained results are correlated with optical properties. It has been shown that annealing at 900 °C leads to the formation of mixed Si-Ce rich clusters. The Ce-related luminescence has been shown to quench between the as-deposited and annealed samples at 900 °C and 980 °C due to the clustering of Ce-ions. At higher annealing temperatures (1100 °C), our characterizations revealed the formation of cerium silicate clusters located at the immediate vicinity of pure Si-ncs. The PL intensity rises substantially as the annealing temperature reaches 1100 °C. This reappearance of PL at high temperature corresponds to the formation and growth of cerium disilicate phase ($Ce_2Si_2O_7$) as detected in APT analysis. Cerium disilicate ($Ce_2Si_2O_7$) seems to be an interesting compound for the development of blue light emitting diodes fully compatible with the silicon technology.

ACKNOWLEDGMENTS

The author thanks the "Région Haute-Normandie" for the financial support of G. Beainy.

[1]L. T. Canham, Appl. Phys. Lett. **57**, 1046 (1990).
[2]L. Pavesi, L. Dal Negro, C. Mazzoleni, G. Franzò, and F. Priolo, Nature **408**, 440 (2000).
[3]L. Dal Negro, M. Cazzanelli, L. Pavesi, S. Ossicini, D. Pacifici, G. Franzo, F. Priolo, and F. Iacona, Appl. Phys. Lett. **82**, 4636 (2003).
[4]M. Fujii, M. Yoshida, Y. Kanzawa, S. Hayashi, and K. Yamamoto, Appl. Phys. Lett. **71**, 1198 (1997).
[5]P. G. Kik, M. L. Brongersma, and A. Polman, Appl. Phys. Lett. **76**, 2325 (2000).
[6]E. Steveler, H. Rinnert, and M. Vergnat, J. Appl. Phys. **110**, 113518 (2011).
[7]A. H. Morshed, M. E. Moussa, S. M. Bedair, R. Leonard, S. X. Liu, and N. El-Masry, Appl. Phys. Lett. **70**, 1647 (1997).
[8]W. C. Choi, H. N. Lee, E. K. Kim, Y. Kim, C.-Y. Park, H. S. Kim, and J. Y. Lee, Appl. Phys. Lett. **75**, 2389 (1999).
[9]J. Li, O. Zalloum, T. Roschuk, C. Heng, J. Wojcik, and P. Mascher, Appl. Phys. Lett. **94**, 011112 (2009).
[10]L. Kepinski, D. Hreniak, and W. Strek, J. Alloys Compd. **341**, 203 (2002).
[11]G. Malashkevich, E. Poddenezhny, I. Melnichenko, and A. Boiko, J. Non-Cryst. Solids **188**, 107 (1995).
[12]N. Chiodini, M. Fasoli, M. Martini, E. Rosetta, G. Spinolo, A. Vedda, M. Nikl, N. Solovieva, A. Baraldi, and R. Capelletti, Appl. Phys. Lett. **81**, 4374 (2002).
[13]G. Xu, Z. Zheng, W. Tang, and Y. Wu, J. Lumin. **124**, 151 (2007).
[14]W.-Y. Cong, S.-M. Li, Y.-J. Wang, L. Tao, X.-Y. Liu, and W.-M. Zheng, J. Lumin. **132**, 161 (2012).
[15]P. Pellegrino, B. Garrido, J. Arbiol, C. Garcia, Y. Lebour, and J. R. Morante, Appl. Phys. Lett. **88**, 121915 (2006).
[16]G. Franzò, S. Boninelli, D. Pacifici, F. Priolo, F. Iacona, and C. Bongiorno, Appl. Phys. Lett. **82**, 3871 (2003).
[17]L.-F. Bian, C. G. Zhang, W. D. Chen, C. C. Hsu, and T. Shi, Appl. Phys. Lett. **89**, 231927 (2006).
[18]D. Larson, D. Foord, A. Petford-Long, H. Liew, M. Blamire, A. Cerezo, and G. Smith, Ultramicroscopy **79**, 287 (1999).
[19]E. Talbot, R. Lardé, P. Pareige, L. Khomenkova, K. Hijazi, and F. Gourbilleau, Nanoscale Res. Lett. **8**, 39 (2013).
[20]M. Roussel, E. Talbot, C. Pareige, R. Pratibha Nalini, F. Gourbilleau, and P. Pareige, Appl. Phys. Lett. **103**, 203109 (2013).
[21]M. Thuvander, H.-O. Andrén, K. Stiller, and Q.-H. Hu, Ultramicroscopy **73**, 279 (1998).
[22]J. Weimmerskirch-Aubatin, M. Stoffel, A. Bouché, P. Boulet, M. Vergnat, and H. Rinnert, J. Alloys Compd. **622**, 358 (2015).
[23]M. Roussel, E. Talbot, R. Pratibha Nalini, F. Gourbilleau, and P. Pareige, Ultramicroscopy **132**, 290 (2013).
[24]E. Talbot, R. Lardé, F. Gourbilleau, C. Dufour, and P. Pareige, EPL **87**, 26004 (2009).
[25]M. Roussel, E. Talbot, F. Gourbilleau, and P. Pareige, Nanoscale Res. Lett. **6**, 164 (2011).
[26]F. Iacona, C. Bongiorno, C. Spinella, S. Boninelli, and F. Priolo, J. Appl. Phys. **95**, 3723 (2004).
[27]R. Mullins, S. H. Overbury, and D. R. Huntley, Surf. Sci. **409**, 307 (1998).
[28]F. Vurpillot, A. Bostel, and D. Blavette, Appl. Phys. Lett. **76**, 3127 (2000).
[29]H. Bi, W. Cai, H. Shi, B. Yao, and L. Zhang, J. Phys. D: Appl. Phys. **33**, 2369 (2000).
[30]L. Kepinski, M. Wolcyrz, and M. Marchewka, J. Solid State Chem. **168**, 110 (2002).
[31]J. Weimmerskirch-Aubatin, M. Stoffel, X. Devaux, A. Bouché, M. Vergnat, and H. Rinnert, Phys. Status Solidi **11**, 1630 (2014).